Improving active distribution network operation through DC microgrid reactive power provision

F. Marasciuolo, M. Dicorato, G. Tricarico, G. Forte
Dept. of Electrical and Information Engineering (DEI)
Politecnico di Bari
Bari, Italy
{francesca.marasciuolo, maria.dicorato, gioacchino.tricarico, giuseppe.forte}@poliba.it

A. Borghetti
Dept. of Electrical and Information Engineering
"G. Marconi"
University of Bologna
Bologna, Italy
alberto.borghetti@unibo.it

***Abstract*— The implementation of active distribution networks (ADNs) carries technical challenges for grid operators, calling distributed resources to contribute to grid services for proper integration. In this context, the DC microgrid structure, thanks to a single converter interface to the external grid, could enhance controllability effectively taking part to network operation strategies. This paper assesses the contribution of DC microgrid in improving ADN performance. To this purpose, an optimal day-ahead methodology for operational planning of ADN hosting DC microgrids, enabled to supply active and reactive power to the grid, is proposed. The compliance of DC microgrid support strategies with network targets is assessed by means of a DistFlow quadratic model, addressing voltage deviations and grid power losses. Simulation tests are carried out using the data of a real ADN to assess the exploitation of DC microgrid capabilities.**

Index Terms—dc microgrids, distribution system operation, reactive power control, optimization.

I. Introduction

The diffusion of distributed renewable energy sources, storage systems and electric mobility into medium and low voltage active distribution networks (ADNs) arises technical challenges for distribution system operators [1]. In particular, the intermittency of renewable generation and electric mobility needs strongly affects peak demand [2] and loss increase [3], along with voltage and frequency fluctuations [4], that should be monitored and mitigated by DSOs. With the aim of ensuring ADN correct and safe operation, regulation of reactive power supply via inverter-based resources represents a promising solution [5] [6], thanks to the controllability within capability region. In this context, microgrid frameworks, combining renewable sources, storage and electric vehicles (EVs) [7], and implementing management strategies for the operation of their facilities, play an important role in power provision to the ADN. Examples are provided in [8], where a two-stage voltage control method that accounts for reactive power incentive is applied to an ADN integrating with multi-microgrid systems, and in [9] and [10] where model predictive control strategies are carried out to for enhancing network security using local controllers for photovoltaic sources (PVs) and EVs.

DC microgrids, viable for the integration of PV, EVs and battery energy storage systems, reveal promising for supporting grid operation. Through the grid connection by means of an AC/DC converter, they are able to provide independent active and reactive power regulation consistent to the converter capability [11], entrusting control actions to a single interface device. Some studies pointed out that DC microgrids interfaced with AC networks can provide significant reactive power regulation by increasing EV participation in the DC microgrid, with a reduction in exchanged active power through the interface converter [12] [13]. Soft open point adoption in DC microgrid improves the percentage of total restored load with respect to classical reconfiguration model after a contingency, enhancing voltage profiles with deviation reduction [14]. Moreover, in [15] voltage regulation in the presence of load increase is implemented by DC microgrid-fed STATCOM.

This paper deals with the ability of DC microgrid to enhance distribution network operation performances through the provision of active and reactive power. To this purpose, a day-ahead optimal programming procedure for ADN operation planning, hosting DC microgrids, is proposed. The procedure employs a second order cone programming problem (SOCP) for minimizing grid loss, adopting the DistFlow ADN model. DC microgrid contributions in ADN are determined by active power exchanges, obtained from local scheduling and reactive power provision by exploiting the reactive support capabilities of the AC/DC converter. The methodology is tested on real data of an existing ADN, by adding several DC microgrids with features obtained from a real demonstrator. The main contributions are summarized as:

- Reactive power provision by DC microgrids, by integrating different resources through converter capability and inspecting its impact on a complete ADN representation.
- Different grid support strategies by DC microgrids are investigated, accounting for internal and grid level uncertainties.
- Simulations consider actual features of ADN and DC microgrids and grid code requirements, considering a

This document has been created in the context of the ECS4DRES project. ECS4DRES is supported by the Chips Joint Undertaking under grant agreement number 101139790 and its members, including the top-up funding by Germany, Italy, Slovakia, Spain and The Netherlands.

979-8-3315-8138-1

case study based on a real medium voltage distribution network.

II. Methodology

The methodology is used to analyze the different operating strategies by the ADN operator considering interaction with microgrids. Two different approaches for DC microgrid integration are analyzed, as sketched in Figure 1.

In Approach 1, the operation of DC microgrid is devoted to grid support, being embedded in the ADN problem with objective function OF. The model based on DistFlow determines network operation along with the active and reactive power profiles of all DC microgrids $P_{mg,l}$ and $Q_{mg,l}$.

In Approach 2, each DC microgrid, involving PV and EVs, pursues local objective by solving a local optimization problem with objective function OF_{mg} minimizing the energy procurement costs linked to the active power exchange level and considering internal needs. In particular, uncertainties related to the forecast of PV production and EV charge levels are taken into account by means of a chance-constrained approach, providing up and down reserve levels within the DC microgrid, as described in [7][20][21]. This provides exchanged active power $P_{mg,l}$ to the ADN problem, obtaining network operation along with DC microgrid exchanged reactive power $Q_{mg,l}$.

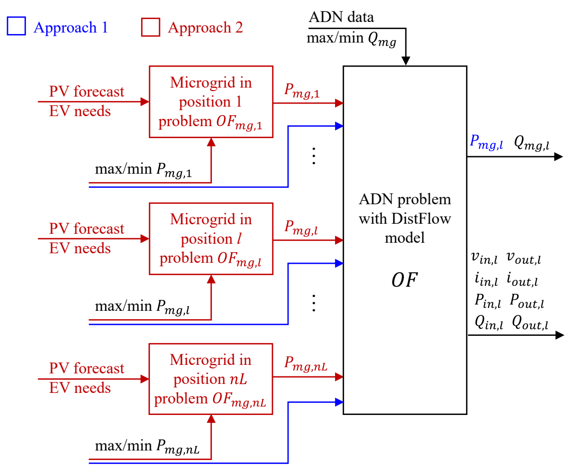

Figure 1. Scheme of the DC microgrid integration approaches.

The methodology for the radial distribution network employs the DistFlow-based optimization problem, as described in [16]. The direction of power flow from the external high voltage network to the terminal nodes is assumed as reference. The set of the buses and branches have the same cardinality nL and the associate index is l. The total number of timesteps is T, representing equal time intervals with duration Δt. Each branch is represented by means of two longitudinal impedances (half the line impedance $z_l = r_l + jx_l$) and a shunt admittance (equal to line admittance jb_l) in the T-model with single sending and receiving buses. Loads and generators are connected to the receiving buses of each line. A schematic representation of the branch model is reported in Figure 2. For each timestep t, the main variables are: input active and reactive powers, $P_{in,l,t}$ and $Q_{in,l,t}$, output active and reactive powers towards the adjacent line ($P_{out,l,t}$ and $Q_{out,l,t}$), squared values of starting and ending nodal voltages $v_{in,l,t}$ and $v_{out,l,t}$, along with squared values of input and output line currents $i_{in,l,t}$ and $i_{out,l,t}$. With the aim of taking into account capacitance effect on the distribution feeders, the squared voltage in the middle point is also considered $v_{mp,l,t}$, as well as power levels $P_{mp,l,t}$ and $Q_{mp,l,t}$. Variables $P'_{out,l,t}$ and $Q'_{out,l,t}$ represent the active and reactive powers in the line before the effect of the local loads/generators. $P_{load,l,t}$ and $P_{gen,l,t}$ are respectively the power demand by the load and the sum of power produced by the generators located in the same node. Same considerations hold for demanded and generated reactive powers.

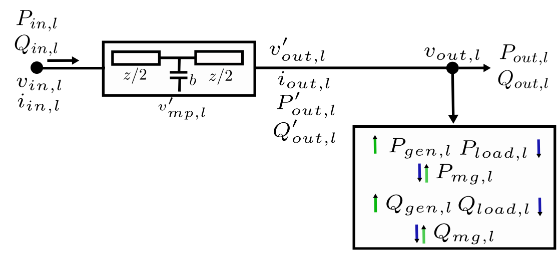

Figure 2. Model of the generic network line in generic timestep t.

The model is summarized by (1)-(9), taking into account the relationships between bus voltage drop and active and reactive flows, along with coupling constraints of nodal voltage, input and output active/reactive powers of adjacent lines.

$$v_{mp,l,t} = v_{in,l,t} - r_l \cdot P_{in,l,t} - x_l \cdot Q_{in,l,t} + 0.25 \cdot (r_l^2 + x_l^2) \cdot i_{in,l,t} \tag{1}$$

$$v_{in,l,t} - v'_{out,l,t} = 2 \cdot r_l \cdot P_{in,l,t} + 2 \cdot x_l \cdot Q_{in,l,t} - 0.75 \cdot (r_l^2 + x_l^2) \cdot i_{in,l,t} - 0.25 \cdot (r_l^2 + x_l^2) \cdot i_{out,l,t} + x_l \cdot b_l \cdot v_{mp,l,t} \tag{2}$$

$$P_{in,l,t} = P'_{out,l,t} + 0.5 \cdot r_l \cdot i_{in,l,t} + 0.5 \cdot r_l \cdot i_{out,l,t} \tag{3}$$

$$Q_{in,l,t} = Q'_{out,l,t} - b_l \cdot v_{mp,l,t} + 0.5 \cdot x_l \cdot i_{in,l,t} + 0.5 \cdot x_l \cdot i_{out,l,t} \tag{4}$$

$$P'_{out,l,t} = P_{out,l,t} + P_{load,l,t} - P_{gen,l,t} + P_{mg,l,t} \tag{5}$$

$$Q'_{out,l,t} = Q_{out,l,t} + Q_{load,e,t} - Q_{gen,e,t} + Q_{mg,l,t} \tag{6}$$

$$v_{in,l,t} = v_{out,l+1,t} = v_{n,t} \tag{7}$$

$$\sum_{k \in \Omega s,i} P_{out,k,t} = \sum_{k \in \Omega r,i} P_{in,k,t} \tag{8}$$

$$\sum_{k \in \Omega s,i} Q_{out,k,t} = \sum_{k \in \Omega r,i} Q_{in,k,t} \tag{9}$$

where $\Omega_{s,i}$ and $\Omega_{r,i}$ indicate the sets of branches that have bus i as the sending and receiving bus, respectively. The integration of DC microgrids within the distribution network implies the introduction in (5) and (6) of exchanged active and reactive power at the interface through the AC/DC converter, namely $P_{mg,t}$ and $Q_{mg,t}$. It is assumed that positive values of the quantities correspond to power absorption (load behavior of the microgrid), whereas negative values to generator behavior. Equality constraints between apparent power and squared

979-8-3315-8138-1

values of voltages and currents are relaxed in cone constraints (10)-(13). Constraints (14)-(16) link the power at the middle point of the line with currents and input/output powers.

$$P_{in,l,t}{}^2 + Q_{in,l,t}{}^2 \le v_{in,l,t} \cdot i_{in,l,t} \tag{10}$$

$$P_{mp,l,t}{}^2 + Q'_{mp,l,t}{}^2 \le v_{mp,l,t} \cdot i_{in,l,t} \tag{11}$$

$$P_{mp,l,t}{}^2 + Q_{mp,l,t}{}^2 \le v_{mp,l,t} \cdot i_{out,l,t} \tag{12}$$

$$P'_{out,l,t}{}^2 + Q'_{out,l,t}{}^2 \le v'_{out,l,t} \cdot i_{out,l,t} \tag{13}$$

$$P_{mp,l,t} = P'_{out,l,t} + 0.5 \cdot r_l \cdot i_{out,l,t} \tag{14}$$

$$Q_{mp,l,t} = Q'_{out,l,t} + 0.5 \cdot x_l \cdot i_{out,l,t} \tag{15}$$

$$Q'_{mp,l,t} = Q_{mp,l,t} - b_l \cdot v_{mp,l,t} \tag{16}$$

The feasibility of the constraint relaxation is successively assessed by checking the mismatch to be lower than a specific small tolerance, with a post-optimization procedure. Upper and lower bounds are set for all the optimization variables according to the technical features of the distribution network feeders and microgrid components. In particular, AC/DC converter capability is set, posing reactive power limits at different active power levels. Objective function OF considers the distribution network viewpoint, represented by the daily active power loss minimization, expressed as in (17).

$$OF = \sum_{t}^{T} \sum_{l}^{nL} 0.5 \cdot r_l \cdot i_{in,l,t} + 0.5 \cdot r_l \cdot i_{out,l,t} \tag{17}$$

III. CASE STUDY

The considered ADN case study involves six MV feeders connected to a 132/15 kV substation with three transformers for a total of 100 MVA, located in the city of Modena (Italy). The system includes 135 buses and 134 branches. The time horizon considered is one day with 15-minutes intervals ($T = 96$). The load active and reactive load daily profiles are shown in Figure 3, with peak values of 16.38 MW and 7.93 Mvar, and a total energy demand of 267.9 MWh and 129.7 Mvarh. The ADN integrates 3 synchronous generators (SG) and 35 PV plants, generating 11.4 MWh and 5.9 MWh respectively [17]. The integrated DC microgrid model includes 20 kWp PV generator, a 25 kW/90 kWh BESS, a set of 5 V2G-enabled EV stations of 15 kW and one 70 kW EV fast-charging station, with the characteristics of a real demonstrator located in Bari (Italy) [7]. Maximum values of active power at grid connection point is set to 50 kW, and maximum reactive power is set to ±24.2 kvar – corresponding to a power factor 0.9 at maximum active power – for all active power levels, according to Italian distribution grid code capability curve required [18] [19]. A total of 136 DC microgrids are spread over 68 buses of the ADN as shown in Figure 4 (considering two microgrids in each node), for a maximum total contribution of 6.8 MW and 3.29 Mvar, nearly 40% of the demand peak power.

Scenario 1 is based on Approach 1, and Scenario 2 correspondently accounts for Approach 2, where active power exchanges of DC microgrids with the ADN derive from procedures in [7] and [20], which account for reserve levels to cope with PV uncertainties with a 95% probability, and statistically reproduced with a multivariate normal distribution. Scenario 2b is analyzed with the same assumptions of Scenario 2 but neglecting reactive power contribution by DC microgrids.

Moreover, in Scenario 2, in order to assess how DC microgrid flexibility performs in the presence of grid load forecast errors, a Monte Carlo analysis is carried out with the simulation of 100 scenarios accounting for a normal distribution with 4% standard deviation for active power, keeping constant power factor.

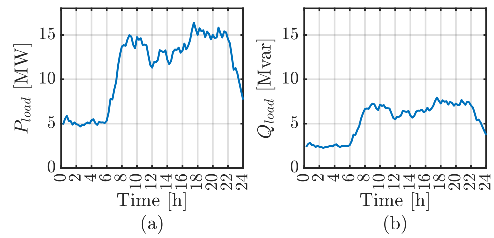

Figure 3. Total active and reactive load power.

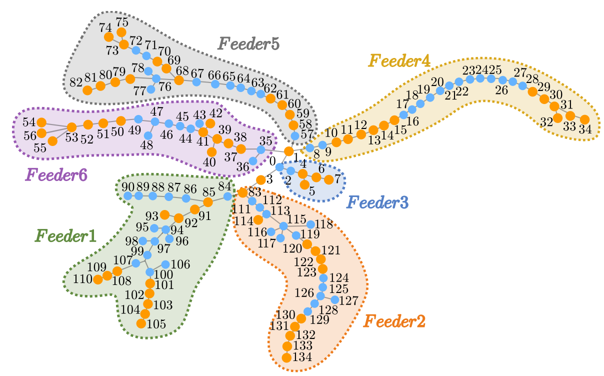

Figure 4. Integration of DC microgrids within the distribution network.

IV. RESULTS

Simulations are carried out using YALMIP tool in Matlab environment, and with MOSEK solver for the SOCP problem, with an average computational time of 6 minutes for the whole daily schedule.

A. Scenario 1 (Approach 1)

The active power exchanges in the ADN are shown in Figure 5.a, with positive values representing generated power and negative values for demand. The contribution of DC microgrids, especially in the horizon 00:00-06:00 is significant, supplying almost the total load demand, and modulated according to microgrid position in the network. The contribution in active power provision is still present during the following hours, though not covering total load, as the power at the slack bus (connection with the upstream network) starts to grow, along with the generated power of PV plant. The same consideration applies for reactive power exchanges, shown in Figure 5.b. DC microgrids contribute with maximum reactive power provision when the load increases. The difference between generation and load is due to reactive power in network elements.

The effect on the grid is depicted by nodal voltages in Figure 6, as they keep the value 1 p.u. in the time interval 00:00-06:00

979-8-3315-8138-1

in all feeders. Feeder 3 keeps nodal voltages greater than 0.99 p.u., due to its short length, whereas further nodes in feeder 4 reach voltages lower than 0.98 p.u. in the evening.

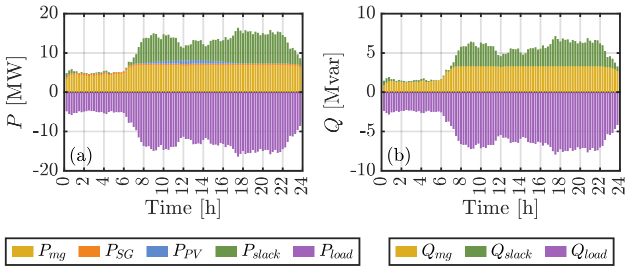

Figure 5. Scenario 1. Grid active power (a) and reactive power (b) exchanges.

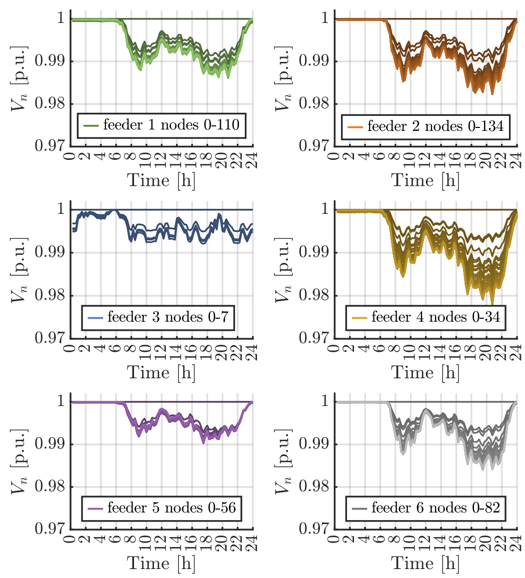

Figure 6. Scenario 1. Nodal voltages.

B. Scenario 2 (Approach 2)

For Scenario 2, different active power exchanges are shown in Figure 7.a. DC microgrid contributions are limited, as provided by the daily local operations that each DC microgrid implements to achieve the local targets. DC microgrids behave as loads at their maximum power during the 02:00-07:00 and 10:00-12:00 intervals, as well as at 16:00. They are only able to supply power to the ADN during the evening hours, when local internal resources are available. For reactive power provision, considerations of Scenario 1 also apply to Scenario 2, since it is bound by the grid code capability curve at a constant value, irrespective of active power level. Hence, especially with high demand, DC microgrids supply their maximum reactive power (Figure 7.b). The profiles of Scenario 2b are analogous in active power and are covered only by slack bus in reactive power, therefore they are not reported. Nodal voltages, not reported for purpose of brevity, are higher than 1 p.u. when load demand is low (interval 00:00-06:00) and reactive power by microgrids supplies almost the totality of the load. However, during the day, the increase of load due to DC microgrids leads to an overall reduction of nodal voltages, especially at the terminal nodes of the feeders.

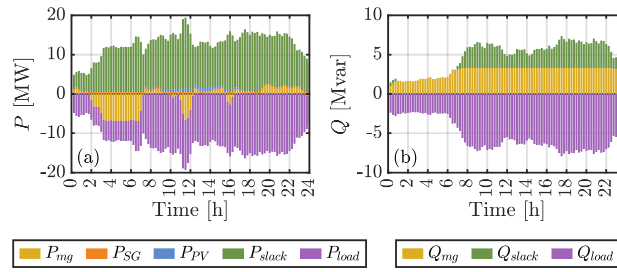

Figure 7. Scenario 2. Grid active power (a) and reactive power (b) exchanges.

C. Scenario comparison

The comparative analysis between scenarios is based on nodal voltage deviations from the values in Scenario 0 (which assumes the absence of DC microgrids). Figure 8 shows the average percentage voltage deviations for each feeder in the three scenarios. With the exception of feeder 3, Scenario 1 yields higher advantages than Scenario 2, due to the greater capability of DC microgrid in both active and reactive power supply. In Scenario 2b, however, voltage profiles worsen in the first hours, due to the increasing power demand of DC microgrids, and improve slightly in the evening.

Regarding total network losses, Scenario 1 shows an 85% reduction compared to Scenario 0, whereas Scenario 2 shows a 47% reduction (see Table I). These results indicate a positive impact of DC microgrids on network operational performance. However, Scenario 2b shows a lower loss reduction (21%), highlighting the pursuit of the objective while limiting positive network impact due to the absence of reactive power provision.

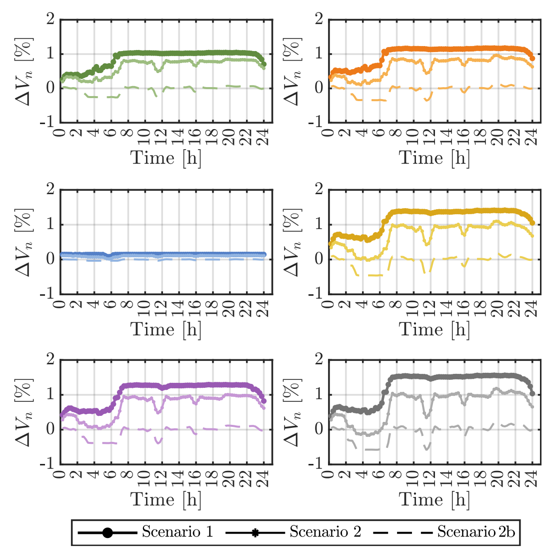

Figure 8. Medium nodal voltage deviations of Scenario 1, Scenario 2 and Scenario 2b and w.r.t. Scenario 0, for each network feeder.

TABLE I. TOTAL NETWORK LOSSES IN ALL SCENARIOS

Scenario	Total losses [MWh]
0	1.960
1	0.292
2	1.045
2b	1.556

979-8-3315-8138-1

D. Monte Carlo analysis

The impact of load forecast uncertainties is investigated by the Monte Carlo analysis based on Scenario 2. The resulting daily voltage profiles of feeder 6 (as average among nodes) are shown in a boxplot for each time step in Figure 9. Nodal voltage average values are higher than 0.97 p.u. throughout the feeder in every scenario analyzed and distributions show a maximum variation of 0.018 p.u. in the evening, though interquartile range does not exceed 0.006 p.u.. Similar results are obtained for the other feeders. For daily active losses, an average value of 1.0132 MWh is detected with a standard deviation of 0.074 MWh (nearly 7%), which is in line with Scenario 2 results.

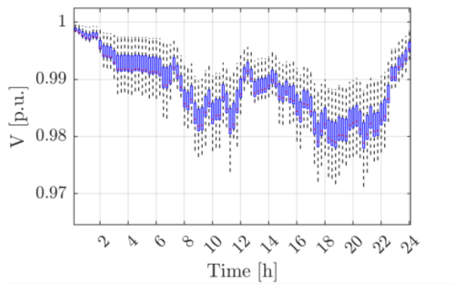

Figure 9. Average nodal voltage of feeder 6 with Monte Carlo analysis.

V. Conclusion

This paper has proposed a procedure for assessing the contribution of DC microgrids to ADN operation through coordinated active and reactive power provision, based on a day-ahead optimal programming framework that integrates local DC microgrid scheduling with grid-level optimization, formulated as a second-order cone programming problem.

Simulation results on a real ADN have demonstrated that DC microgrids can significantly enhance network performance by providing both active and reactive power. When DC microgrids are completely devoted to grid support, network losses have decreased by up to 85% compared with the reference case, and voltage profiles have remained closer to nominal values across all feeders. In case local DC microgrid resources are prioritized, smaller improvements in voltage regulation and a 47% reduction in losses have been observed. However, even considering grid load variation, DC microgrid contributions still lead to significant improvements of grid operation performance. The analysis has shown the importance of coordinating operation between grid and microgrid operators. Even limited DC microgrid participation can improve voltage stability and loss reduction, and the flexibility is valid even with grid load errors.

Future work will address the coordination between local DC microgrid control and the ADN one, in a hierarchical framework, as well as the interaction among multiple interconnected microgrids, and the real-time control strategies.

References

[1] I. Alvarez-Fernandez et al., "Impact analysis of DERs on bulk power system stability through the parameterization of aggregated DER_a model for real feeders," Electric Power Systems Research, vol. 189, p. 106822, 2020.

[2] L. Wang, Z. Qin, T. Slangen, P. Bauer T. van Wijk, "Grid Impact of Electric Vehicle Fast Charging Stations: Trends, Standards, Issues and Mitigation Measures - An Overview," in IEEE Open Journal of Power Electronics, vol. 2, pp. 56-74, 2021.

[3] N. Kebir, M. Maaroufi, "Technical losses computation for short-term predictive management enhancement of grid-connected distributed generations," Renewable and Sustainable Energy Reviews, vol. 76, pp. 1011–1021, 2017.

[4] J. P. Carvallo et al., "A framework to measure the technical, economic, and rate impacts of distributed solar, electric vehicles, and storage," Applied Energy, vol. 297, p. 117160, 2021.

[5] X. Ma, X. Zhou, W. Wang, "Voltage Control Strategy of Active Distribution Network Considering Reactive Power Margin of Photovoltaic Inverter," *2024 China Automation Congress (CAC)*, Qingdao, China, 2024, pp. 1495-1500.

[6] Y. Zou, Y. Xu, "DER-Inverter Based Reactive Power Ancillary Service for Supporting Peer-to-Peer Transactive Energy Trading in Distribution Networks," *IEEE Trans. Pow. Syst.*, vol. 40, no. 1, pp. 753-764, 2025.

[7] M. Dicorato, G. Forte, F. Marasciuolo, M.C. Cavarretta D. De Michino, "Integration of EV fast charging station into a DC-based microgrid", *IEEE Trans. on Ind. Appl.*, vol. 61, no. 4, Jul.Aug. 2025, pp. 5560-5570.

[8] K. Zhang, J. Chen, X. Qi, Y. Chen, Z. Sun, M. Wei, "Two-Stage Voltage Control Strategy for Distribution Networks with Multi-Microgrids Considering Reactive Power Incentive," *2024 IEEE I&CPS Asia*, Pattaya, Thailand, 2024, pp. 169-174.

[9] M.R. Dar, S. Ganguly, "A Hybrid Control Scheme for Voltage Regulation and Energy Loss Minimization in Active Distribution Networks Based on Model Predictive Control," *2024 IEEE PES ISGT Asia*, Bengaluru, India, 2024, pp. 1-6.

[10] L. Wang, A. Dubey, A. H. Gebremedhin, A. K. Srivastava, N. Schulz, "MPC-Based Decentralized Voltage Control in Power Distribution Systems With EV and PV Coordination," in *IEEE Transactions on Smart Grid*, vol. 13, no. 4, pp. 2908-2919, July 2022.

[11] J. Ding, B. Peng, X. Zong, W. Yuan, Y. Yang and W. Zeng, "Analysis on the Reactive Power Regulation of Inverter and Voltage in Distribution Network," *IEEE CIEEC conf.*, Harbin, China, 2024, pp. 3559-3564.

[12] A. Safari and H. Rahbarimagham, "An Improved Control Strategy for Managing Reactive Power and Reducing Capacity of Interlinking Converters by Participating of Electric Vehicles in Hybrid AC/DC Microgrids,", IEEE Access, vol. 13, pp. 17878-17894, 2025.

[13] R. A. Núñez-Rodríguez, C. Unsihuay-Vila, J. Posada, O. Pinzón-Ardila, "Data-Driven Distributionally Robust Optimization for Day-Ahead Operation Planning of a Smart Transformer-Based Meshed Hybrid AC/DC Microgrid Considering the Optimal Reactive Power Dispatch," Energies, vol. 17, no. 16, p. 4036, 2024.

[14] I.I. Picioroaga, A.M. Tudose, D.O. Sidea, C. Bulac, "Supply Restoration in Active Distribution Networks Based on Soft Open Points with Embedded DC Microgrids," Mathematics, vol. 10, no. 2, p. 211, 2022.

[15] F. M. Khater et al., “Voltage Control of a Three-Phase Distribution Grid using a DC Microgrid-Fed STATCOM”, Eng. Technol. Appl. Sci. Res., vol. 14, no. 1, pp. 12966–12974, Feb. 2024.

[16] T. Harighi, A. Borghetti, F. Napolitano, F. Tossani, "Provision of reactive power services by energy communities in MV distribution networks", Sustainable Energy, Grids and Networks, Volume 34, pp. 101038, 2023.

[17] T. Harighi, et al., "Quantifying maximum limits for reactive power flexibility provision in energy communities: A case study of a real distribution power network." *Proc. Int. Conf. CIGRE*. 2024.

[18] Italian Standard CEI, “CEI 0-16. Reference technical rules for the connection of active and passive consumers to the HV and MV electrical networks of distribution Company”, V5, 2025 (in Italian).

[19] Italian Standard CEI, “CEI 0-21. Reference technical rules for the connection of active and passive users to the LV electrical utilities”, V3, 2025 (in Italian).

[20] F. Marasciuolo, M. Dicorato, G. Tricarico, G. Forte, R. Sbrizzai, "Demand Response in Distribution Operation Planning Hosting DC Microgrid-Based Energy Community," *2025 EEEIC / I&CPS Europe*, Chania, Crete, Greece, 2025, pp. 1-6.

[21] F. Marasciuolo, C. Orozco, M. Dicorato, A. Borghetti, G. Forte, "Chance-constrained calculation of the reserve service provided by EV charging station clusters in Energy Communities," IEEE Transactions on Industry Applications, vol. 59, no. 4, pp. 4700-4709, July-Aug. 2023.